Sensor and Simulation Notes
Note 563
June 2013

Selection of Ideal Feed profile for Asymptotic Conical Dipole Fed Impulse Radiating Antenna

Dhiraj K. Singh[1], D. C. Pande[1], and A. Bhattacharya[2], Member, *IEEE*

[1]Electronics & Radar Development Establishment, Bangalore, India
[2]Indian Institute of Technology, Kharagpur, India

This work is an adaptation of the work already published by the same authors in "**Progress in Electromagnetic research C**" Vol.35, 95-109, 2013.

Abstract— Equivalent charge method is used to design ultra wide band asymptotic conical dipole (ACD) antenna. Combination of linear charge density and point charges is used to generate different profiles for ACD antennas. Two different profiles of ACD antenna are used as a feed for reflector based impulse-radiating antennas (IRAs). This paper focuses on the selection of ideal ACD profile as well as the requisite charge distribution for ACD antenna as a feed to design 100Ω input impedance reflector IRA. An ideal Configuration of ACD feeding structure for reflector IRA is chosen based on FDTD analysis results. To validate the utility of the proposed new feed an ACD-fed half IRA is realized with input impedance of nearly 50 Ω. Measurements are carried out using single-ended instrumentation without any impedance adaptor as commonly done with Conventional IRAs.

***Index Terms*— ACD, BALUN, FDTD, IRA, UWB**

1. INTRODUCTION

Biconical structures are know for their wideband characteristics and their different variants have been worked out in past for various antenna geometries. Reflector based ultra wideband (UWB) biconical antennas popularly known as impulse radiating antennas (IRAs) [1]-[6] have been developed for good directional and time domain characteristics. IRAs are commonly designed for 200 Ω input impedance wherein the conical plate transmission line feed used is of 400 Ω. Typically, in an IRA, two 400 Ω conical plate lines are connected in parallel at the feed point to get 200 Ω input impedance.

The reason for choosing a 400 Ω line is to get a smaller cone angle for the transmission line thereby reducing the aperture blockage and, in turn, achieving a better antenna gain. Most of the pulse generators have an unbalanced coaxial output with a 50Ω source resistance. To Connect 50 Ω voltage source to the 200 Ω input of IRA, a 50 Ω to 200 Ω balun is used. ACD fed reflector IRAs [15] shows promise to reduce the input impedance of IRAs without reduction in gain and hence exempts use of 50 Ω to 200 Ω balun.

This paper describes ACD antennas of different profiles generated due to different charge distributions and selection of optimum ACD profile as feed to get a 100 Ω IRA. ACD fed IRA with two different feed profile was analyzed using FDTD and the ideal feed profile was chosen based on these results. The analysis results were validated by doing measurement on realized half IRA (HIRA) of nearly 50 Ω input impedance. In Section 2 of the paper, the design formulas and different profiles for this ACD feed is presented. The time domain analysis of IRA with ACD feed arms with different profile is discussed in Section 3. Time domain measurement results are elaborated in Section 4. Discussion and Conclusion are presented in Section 5 & 6 respectively.

2. FEEDING DIPOLE DESIGN

Equivalent charge method [9,15] is used to generate the profile of the ACD antenna. In the equivalent charge method, a hypothetical static charge distribution is defined with the total charge set equal to zero. This distribution is defined to be rotationally symmetric about *z*-axis with opposite charge reflected about the symmetry plane (*x-y* plane) as shown in Fig. 1. The derivation of potential distribution from this equivalent charge is done using cylindrical (r,φ, z) coordinate systems as shown in Fig.2. Two equipotential surfaces of equal and opposite potentials are thus generated defines the profile of the biconical antenna. Both of these surfaces can be realized by perfect electric conductors with an appropriate total surface charge such that the potential distribution external to the surface remains unchanged.

The equivalent line charge λ(z) and the two point charges Q on the *z*-axis be given by [12]:

$$\lambda(z) = \begin{cases} \lambda_0\ , & 0 < z < z_0 \\ -\lambda_0\ , & 0 > z > -z_0 \\ 0, & z = 0, z > z_0 \end{cases}$$

$$Q = \begin{cases} Q_0\ , & z = z_0 \\ -Q_0\ , & z = -z_0 \end{cases} \qquad (1)$$

where mean charge separation $z_0 > 0$, charge density $\lambda_0 > 0$, and discrete charge $Q_0 > 0$

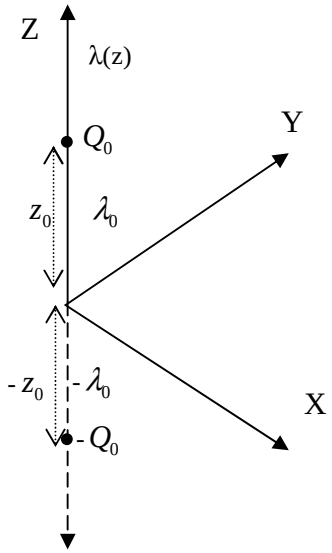

Fig. 1: Charge distribution

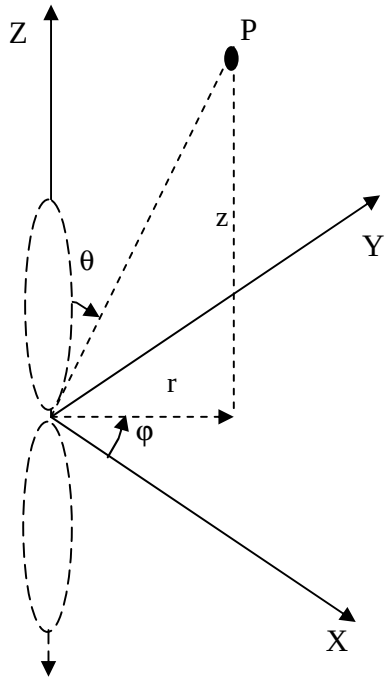

Fig.2: Biconical geometry

In order to generate the ACD profile, we need to find out the ACD countor co-ordinates(r, z). The potential distribution of this charge distribution is the superposition of the potentials from the distributed charges and the point charges. The potential function generated by the line charges is given by equation (2).

Potential distribution due to this equivalent charge distribution, at any point $\mathrm{P}(r,\varphi,z)$ in cylindrical coordinates is

$$\phi_l = \frac{\lambda_0}{4\pi\varepsilon_0} \ln\left\{ \frac{\left[z+\sqrt{z^2+r^2}\right]^2}{\left[z+z_o+\sqrt{(z+z_o)^2+r^2}\right]\left[z-z_o+\sqrt{(z-z_o)^2+r^2}\right]} \right\} \qquad (2)$$

The potential at a point (z, r) due to the two point charges is given by

$$\phi_p = \frac{Q_0}{4\pi\varepsilon_0}\left(\frac{1}{\sqrt{(z-z_0)^2+r^2}} - \frac{1}{\sqrt{(z+z_0)^2+r^2}} \right) \qquad (3)$$

The total charge on the positive line segment is $\lambda_0\ z_0$. A dimensionless quantity α is defined as the ratio of the point charge to the line charge, so that

$$Q_0 = \alpha\ \lambda_0\ z_0 \qquad (4)$$

The summation of potential due to line charge and point charge is equated to the surface potential of an infinite biconical structure. The two equipotential biconical Surfaces are defined as shown in Fig. 2. The surface potential function and characteristic impedance for an infinite biconical structure as derived in Appendix "A".

$$\phi_S = \frac{\lambda_0}{2\pi\varepsilon_0}\ln\left[\cot\left(\frac{\theta_0}{2}\right)\right] \tag{5}$$

$$Z_c = 120\ln(\Theta_0^{-1}) \tag{6}$$

where, $\Theta_0 = \tan(\frac{\theta_0}{2})$

Z_c=Characteristic impedance of infinite bicone in free space.

θ_0 = Bicone angle

When we equate the total potential distribution to that of the infinite bicone ϕ_s, the (z,r) coordinates for the asymptotic conical profiles are given in terms of Θ_0 as

$$\ln\left(\Theta_0^{-2}\right) = \ln\left\{\frac{\left[z+\sqrt{z^2+r^2}\right]^2}{\left[z+z_0+\sqrt{(z+z_0)^2+r^2}\right]\left[z-z_0+\sqrt{(z-z_0)^2+r^2}\right]}\right\} + \frac{\alpha z_0}{\sqrt{(z-z_0)^2+r^2}} - \frac{\alpha z_0}{\sqrt{(z+z)^2+r^2}} \tag{7}$$

The antenna element height is determined by setting $r=0$ at $z=h$, which gives

$$\ln\left(\Theta_0^{-2}\right) = \ln\left(\frac{h^2}{h^2-z_0^2}\right) + \frac{2\alpha z_0^2}{h^2-z_0^2} \tag{8}$$

Where, Θ_0 is a constant determined by the desired asymptotic impedance from the infinite biconical surface [9]. For each value of z between zero and the antenna height h, there exists a unique element radius r. For any given value of $\Theta_0, \alpha,$ and h, equation (8) is solved numerically for z_0 using Newton-Raphson method. Once z_0 and Θ_0 are determined for a particular configuration, Eq. (7) is solved iteratively to get the antenna feed contour for various values of $\alpha,$ as shown in Fig.3**.** The 200 Ω asymptotic conical dipoles for both α = 0 & 1 profiles are individually analyzed without any resistive termination for its return loss with respect to frequency using an excitation source impedance of 200Ω.A gaussian pulse of 50ps full width half maximum (FWHM), 50ps rise time and 0.56 volts peak amplitude as

shown in Fig.13 is used as excitation for simulation. An absorbing boundary condition with seven perfectly matched layers (PML) is used for this simulation.

The calculation of return loss is done for the solid ACD geometry (obtained by rotating the contour of Fig.3 360^0 around the height axis) as well as the ACD plate of length 184mm and 2mm thickness (obtained using a surface profile shown in Fig.3 and its mirror image) for both $\alpha = 0$ & 1 (shown in Fig.4). The return loss plots for the geometries for $\alpha = 0$ and $\alpha = 1$ are shown in Fig.5. and Fig.6. Both of these plots show that solid geometries of both profiles have better impedance matching performance than plates. Though the solid ACD geometry has better impedance matching than plate, still flat ACD is used in this new antenna design to reduce the feed blockage as well as weight of the antenna. The return loss plot as shown in Fig.6. shows less wiggles for ACD solid geometry and there is a marked resonance near 4 GHz. The larger girth of the solid dipole for $\alpha = 1$ profile reduces the inductance, hence wiggles in return loss plot is reduced. The resonance observed near 4 GHz is attributed to the charge separation between point charge and the mean linear charge.

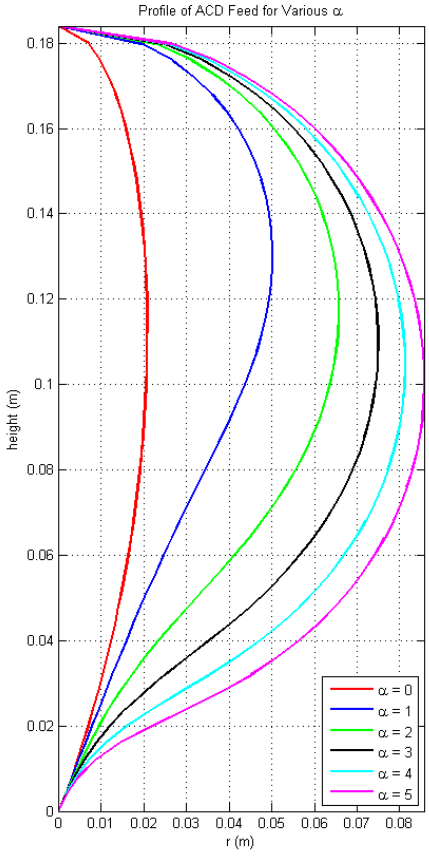

Fig.3: ACD Contours

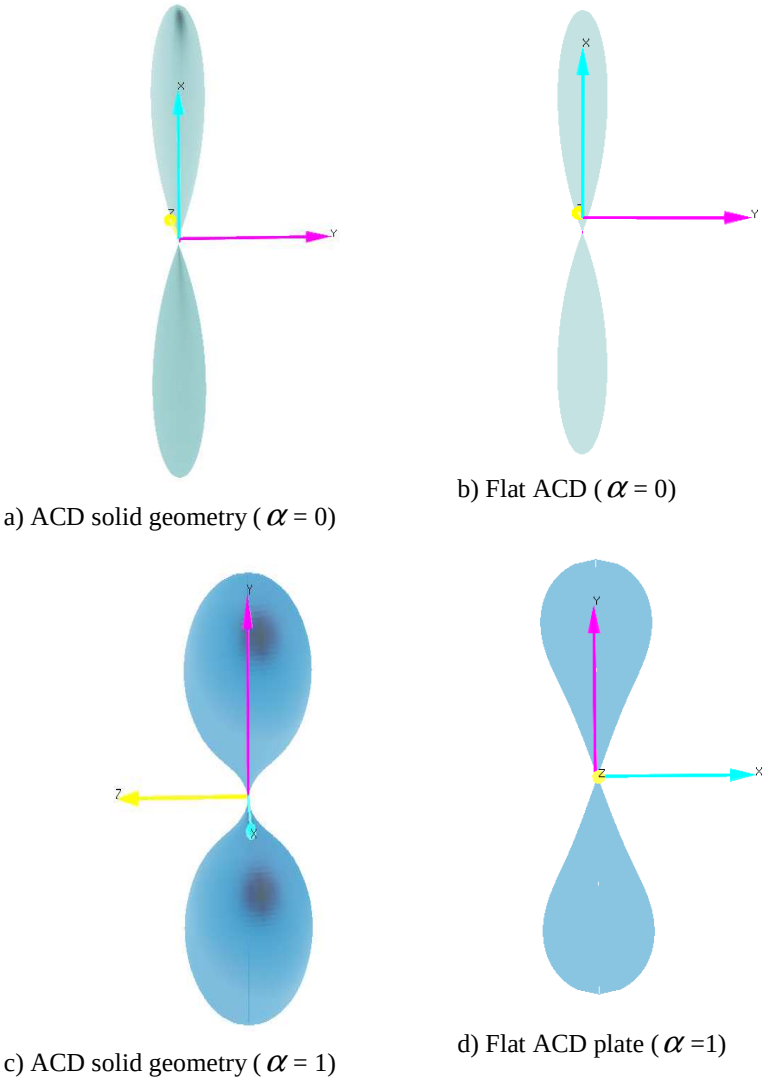

a) ACD solid geometry (α = 0)

b) Flat ACD (α = 0)

c) ACD solid geometry (α = 1)

d) Flat ACD plate (α =1)

Fig.4: ACD geometry profile (α = 0 & 1)

Two asymptotic conical dipole plates out of both these profiles of length 184mm and 2mm thickness were connected in parallel at the feed point to get an input impedance of nearly half the value of the individual dipoles .The combined arms were rotated around the feed point towards the reflector as shown in Fig. 7. The combined feed arms of both profiles are analyzed without reflector and terminating resistors, using excitation source impedance as 100 Ω. A gaussian pulse of 50ps FWHM, 50ps rise time and 0.56 volts peak amplitude as shown in Fig.13 is used as excitation for simulation. An absorbing boundary condition with seven perfectly matched layers (PML) is used for this simulation. The calculated return loss plot of the combined feed arms for both profiles is shown in Fig. 8.

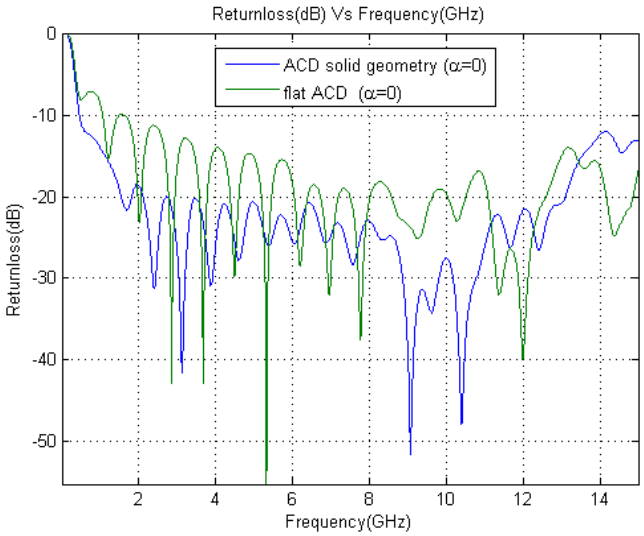

Fig.5: Return loss (dB) Vs Frequency (Hz) (Simulation)

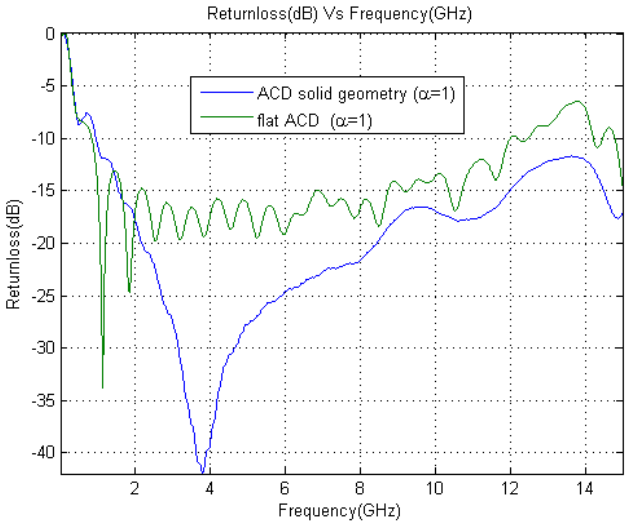

Fig.6: Return loss (dB) Vs Frequency (Hz) (Simulation)

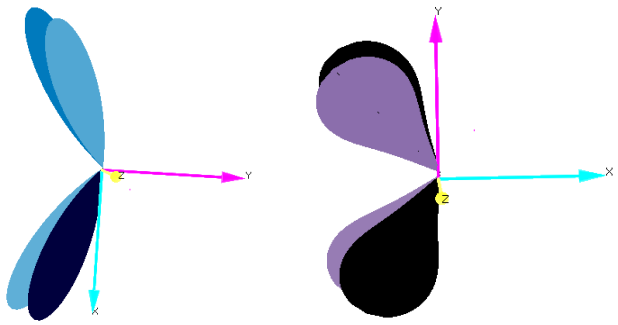

a) ACD feed arms ($\alpha = 0$) b) ACD feed arms ($\alpha = 1$)

Fig.7: Feed arm geometry of ($\alpha = 0$ & 1) profiles

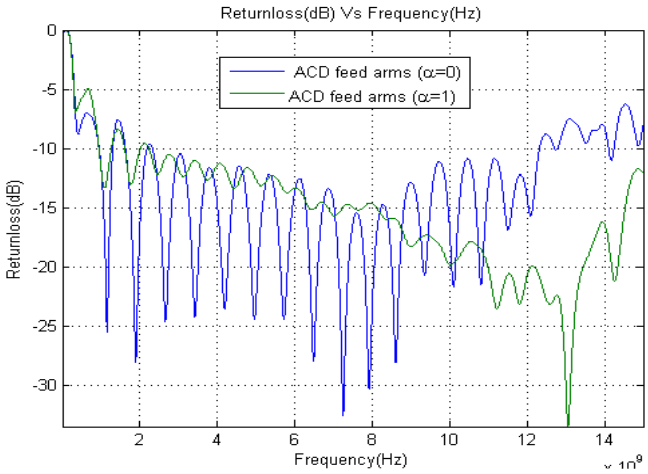

Fig.8: Simulated return loss of ACD feed arms ($\alpha = 0$ & 1)

3. ANTENNA DESIGN AND ANALYSIS

Reflector-based IRAs are designed using a 46 cm diameter parabolic reflector with focal length18.4 cm using the combined flat ACD feed arms of length 184mm and 2mm thickness of both α=0 & 1 profiles as shown in Fig. 9. and Fig.10. Two 200 Ω asymptotic conical dipoles of both profiles connected in parallel at the input of the IRA give a 100 Ω input impedance for the new IRA. Feed arms are placed at ±30 degrees from the vertical axis for both feed profiles. ACD-fed IRA for both the profiles ($\alpha = 0$ & 1) is analyzed in time domain using the finite difference time domain solver XFDTD (v7.1).

The excitation waveform used for the simulation of the antenna is a gaussian pulse of amplitude~ 0.56 volts, FWHM~ 50 ps and rise time~50 ps as shown in Fig. 13. The absorbing boundary condition with seven perfectly matched layers (PML) is used for this simulation. The terminating resistors of 100Ω are placed between each arm ends and the reflector as shown in Fig. 9. and Fig.10. Fig. 11 shows the plot of return loss with respect to frequency for IRAs with different feed. Fig.11 shows that ACD fed IRA (α=1) has better matching at lower frequencies than ACD fed IRA (α=0) because of reduced inductance of the α=1 profile. The return loss of the antenna with feed profile α=0 is better than α=1 at higher

frequencies. The input impedance with respect to frequency is shown in Fig.12. for IRAs with both feed profiles.

The time domain far-zone electric field both E_Θ and E_ϕ (calculated using the excitation signal shown in Fig.13 at bore-sight of the ACD fed IRAs) consists of prepulse, main impulse and post pulse and is shown in Fig.14. Fig.15 shows the time domain far zone response at bore sight for both IRAs. XFDTD (v7.1) solver calculates the far zone electric field at infinity and normalize it to $|r|$=1m. The time domain response of ACD-fed (α=1) is better particularly in late time region but the peak electric field at the bore sight for ACD fed (α=0) IRA is higher than ACD fed (α=1) IRA. The temporal separation observed in the far zone time domain response of the two antennas are due the axial offset of feed arms of ACD fed (α=1) IRA. The gain at bore sight of the ACD fed IRA (α=0) is more than 3dB higher compared to ACD fed IRA (α=1) at high frequencies as shown in Fig.16. ACD fed IRA (α=0) is considered as a favorable choice for fabrication due to higher gain and comparable time domain performance.

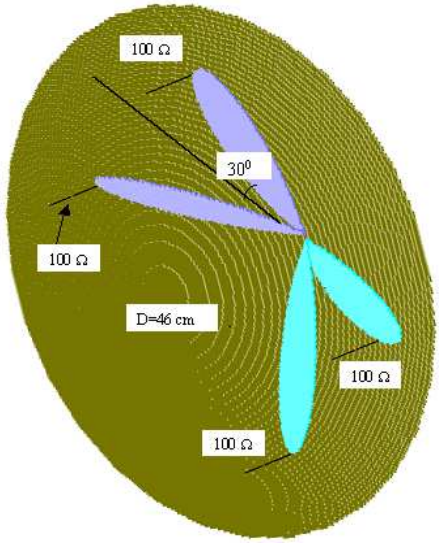

Fig.9: Solid geometry of ACD fed (α=0) IRA

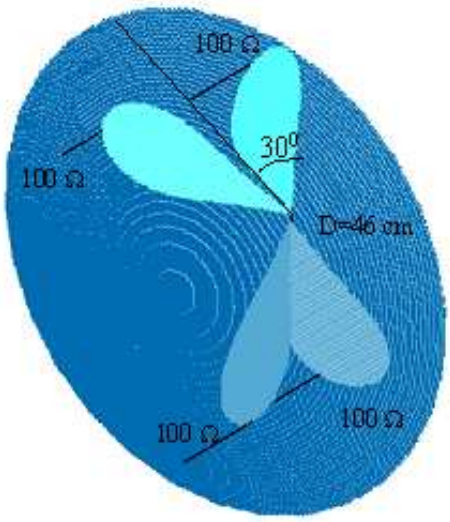

Fig.10: Solid geometry of ACD fed (α=1) IRA

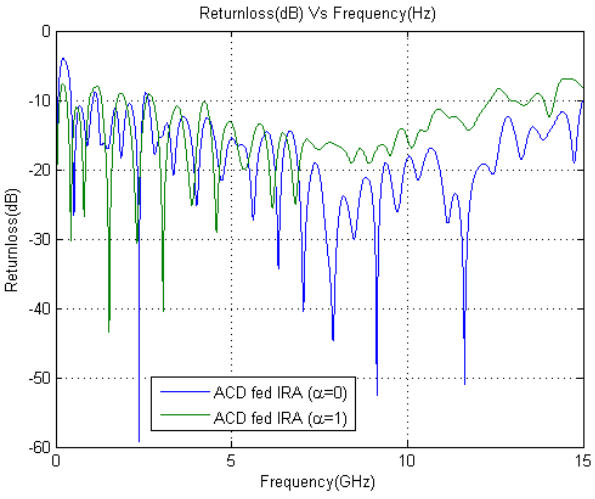

Fig. 11: Simulated Return loss of ACD fed IRA (α=0&1)

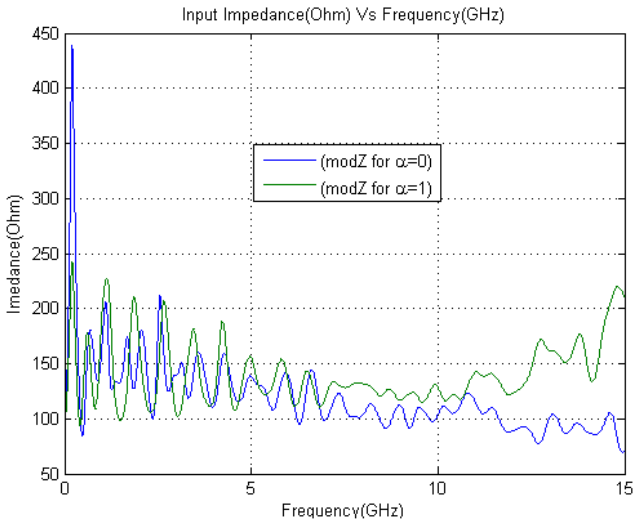

Fig.12**:** Simulated Input Impedance of ACD fed IRA (α=0&1)

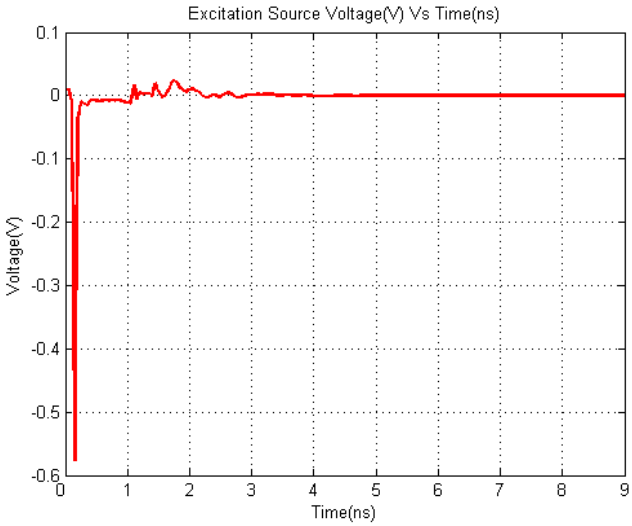

Fig. 13: Excitation impulse signal used for FDTD analysis

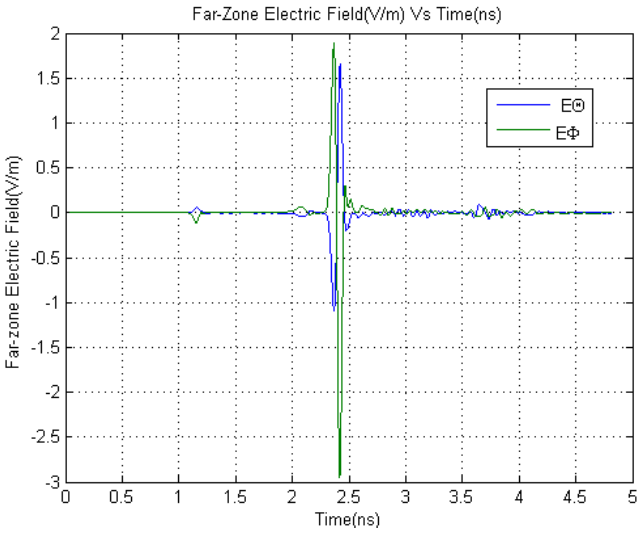

Fig. 14: Far-zone electric field of ACD fed (α =0) IRA

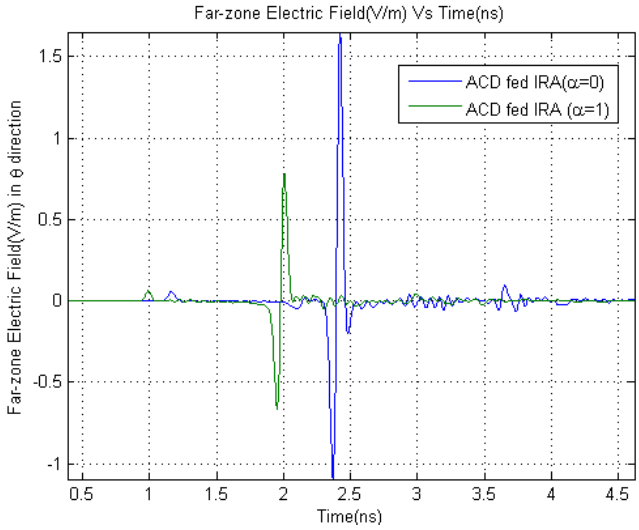

Fig. 15: Far-zone electric field of ACD fed IRAs (α =0&1)

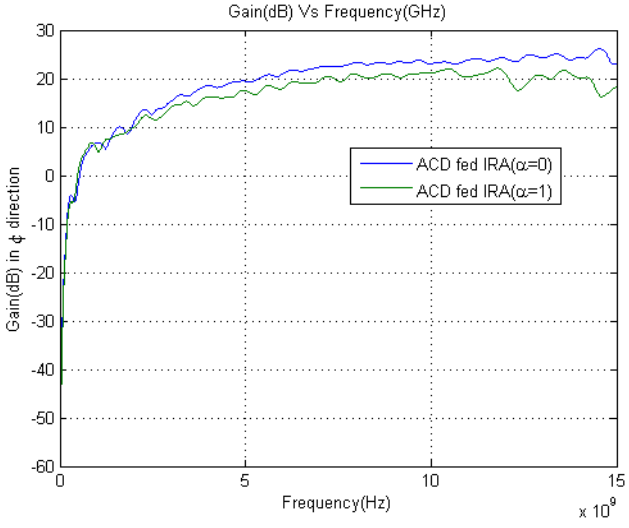

Fig. 16: Gain of ACD fed IRAs (α =0&1) at bore sight

4. EXPERIMENTAL RESULTS

FDTD analysis results show that ACD feed (α =0) profile geometry is ideal for ACD fed reflector IRA. For exciting the designed 100 Ω antenna, either a balun or a differential converter is required. A balun transforms the antenna impedance achieving compatibility with measuring instruments having a 50 Ω impedance. To achieve the same compatibility, a differential converter converts the single ended line to two equal and opposite polarity lines. Therefore, designed antenna was reduced to a half reflector with two arms and a ground plane known as ACD fed half IRA (HIRA). This gave nearly a 50 Ω impedance across the requisite frequency range. The realized ACD-fed (α =0) HIRA is shown in Fig. 17. and its design parameters are given in Table1.1. Return loss of the realized HIRA was measured using agilent PNA E8362B Network analyzer. Return loss versus frequency plot (shown in Fig. 18) shows that return loss is

better than –10 dB in the frequency range of 500MHz to 15GHz. Measured gain of the ACD fed IRA at some of the spot frequencies in the frequency range of 1-15 GHz is shown in Fig.19.

Fig. 17: Realized ACD fed (α =0) HIRA

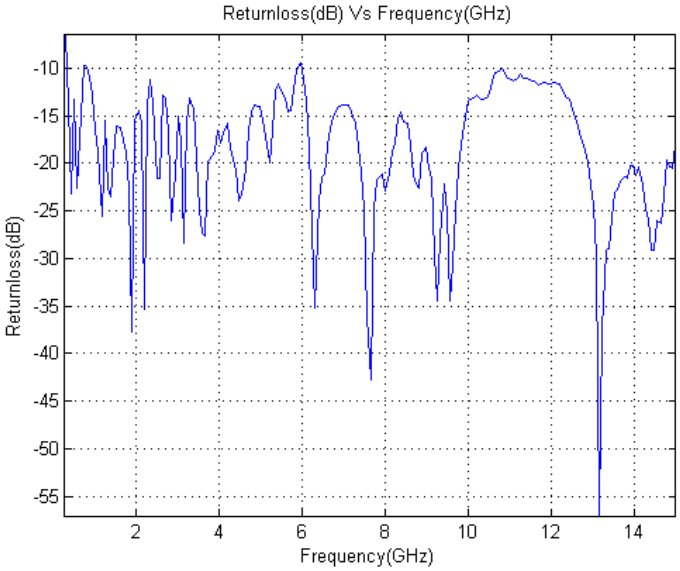

Fig. 18: Measured return loss of ACD-fed (α =0) HIRA

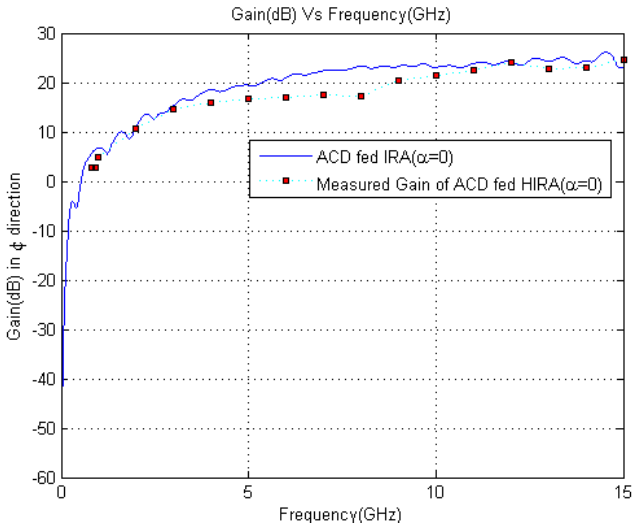

Fig. 19: Measured gain of ACD fed (α =0) HIRA

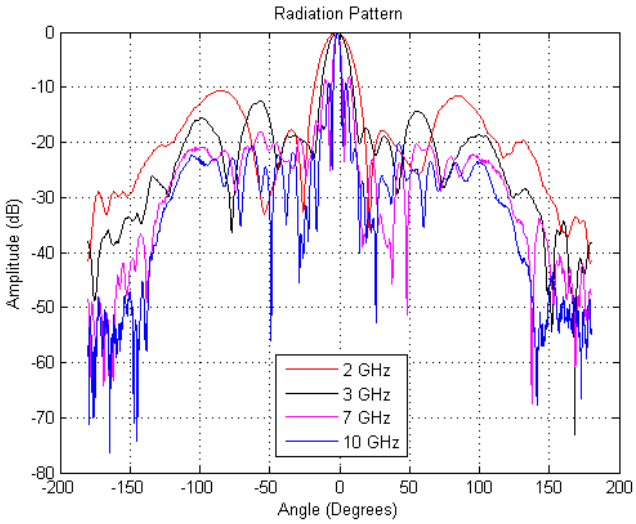

Fig. 20: Measured Radiation Pattern of ACD-fed (α =0) HIRA

Radiation pattern of the antenna is measured at ten different frequencies from 1 GHz to 10 GHz in a near field measurement facility. Fig. 20 shows the measured radiation pattern at 2 GHz, 3 GHz, 7 GHz and 10 GHz.The newly developed ACD-fed (α =0) HIRA is compatible with all the standard instruments as it has nearly 50Ω impedance across the required frequency range. The time domain response of Novel-fed (α =0) HIRA is measured using measurement setup consists of an UWB arbitrary wave generator (AWG) (Tektronix AWG 7122C), an Oscilloscope (Tektronix TDS71604 DPO 16 GHz), ACD sensor (prodyn AD-70D) and balun (prodyn BIB-100F) as shown in Fig.21.The differential output of ACD sensor goes to Oscilloscope through the balun which converts it to single ended with a loss of ~8dB. The sensor output after accounting for the balun loss is used in the eq.8 to obtain peak electric field. The input excitation pulse used for antenna evaluation is a gaussian derivative pulse as shown in Fig.22. The measured time domain

response of the ACD-fed HIRA is first time derivative of the input excitation pulse as shown in Fig.23. The ringing noticed in the antenna response is attributed to the cable pickups.

$$V_0(t) = \vec{A}_e R_0 \varepsilon \frac{\Delta E}{\Delta t} \quad (8)$$

where $\vec{A}_e$=1x10^{-3} m^2= equivalent area of sensor, R_0=100Ω=input resistance of sensor, $V_0(t)$=Sensor output

The simplified analytical expressions for peak electric field $E_p(r)$, peak gain G_p and V_{far} at bore sight of the antenna derived for classical IRA [11] is given in Eq.9-11 respectively. These expressions are used to calculate the stated parameters for ACD feed (α=0) IRA and ACD-fed (α=0) HIRA, though they are derived for IRA with triangular feeding plates separated by 90^0. Antenna parameters for ACD feed (α=0) IRA and ACD-fed (α=0) HIRA, prototype IRA and Jolt [11] is summarized in table 1.1. for reference.

$$E_p(r) = \frac{h_a}{2\pi r c f_g}\left(\frac{dV(t)}{dt}\right)_p \quad \text{(V/m)} \quad (9)$$

$$G_p = \frac{1}{\pi f_g}\left(\frac{h_a}{c t_{mr}}\right)^2 \quad (10)$$

$$V_{far} = rE_p(r) \quad \text{(v)} \quad (11)$$

Where, h_a=equivalent height of antenna f_g= geometrical factor

$V(t)$=Excitation voltage, t_{mr}= max. rate of rise, c= speed of light

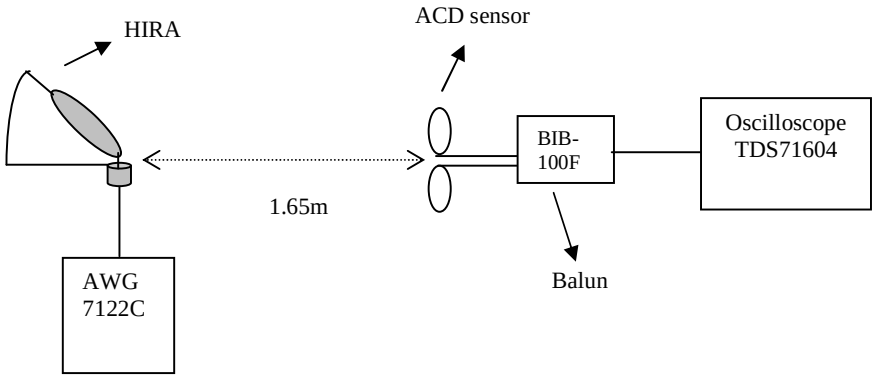

Fig. 21:Time Domain Measurement Setup

The XFDTD solver gives far zone electric field at a distance of 1m, therefore analytical (eq.9) and numerical (FDTD) calculation of peak electric field E_p for ACD feed (α=0) full IRA is done at 1m distance from the antenna. Measurement of electric field for ACD-fed (α=0) HIRA is done at 1.65m from the antenna. The AWG used as source, generates peak pulse voltage of 0.36 v and the sensor used for measurement has very less sensitivity hence the distance for measurement was restricted to 1.65m.The peak

gain in frequency domain for ACD feed (α=0) full IRA and ACD-fed (α=0) HIRA is in close agreement with their peak time domain gain calculated using eq.(10). It is difficult to compare the results obtained with classical IRA's because most of them are built with different dimensions, feed configurations and excitation sources [11].

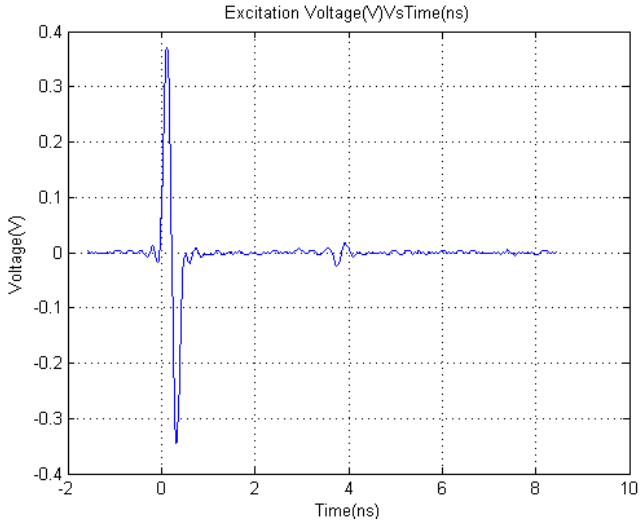

Fig. 22:Excitation signal used for time domain measurement

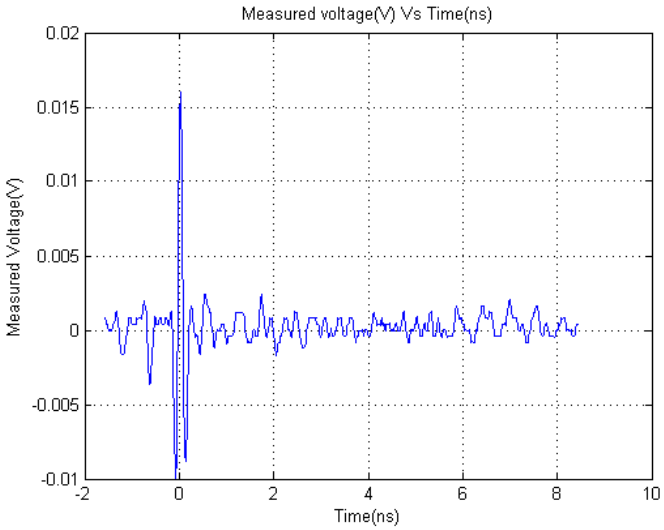

Fig. 23: Measured time domain response of ACD-fed (α=0) HIRA

TABLE1.1 ANTENNA PARAMETERS

Parameter	ACD feed (α=0) full IRA	ACD-fed (α=0) HIRA	Prototype IRA [11]	Jolt [11]
Reflector diameter D	0.46m	0.46m	3.66m	3.048m
Focal length F	184mm	184mm	1.22m	1.158m
F/D	0.4	0.4	0.33	0.375
Number of arms	4	2	4	2
Arm separation	60^0	60^0	90^0	90^0
Input impedance (Ω)	100	50	200	100
Geometrical factor (f_g)	0.265	0.132	0.531	0.265
Peak voltage (V_p)	~0.58 volts	0.36 volts	~120kV	890 kV
Max. rate of rise	~50ps	~50ps	~100ps	~180ps
V_{far}	~7.5 volts	~2.4volts	~1280 kV	~5.4 MV
Gain (G_p)	~564	~71	~2230	~97
G_p (dB)	~27.5 dB	~18.5 dB	~33.4	~20 dB
$E_p(r)$	~5.5 V/m at 1m (Calculation as eq.9)	~1.41 V/m at 1.65m (Calculation as eq.9)	4.2kV/m at 304m[14]	60kV/m at 85m[14]
	~ 3 V/m at 1m (Simulation)	~2.4 V/m at 1.65m (Measured)		

5. DISCUSSION

ACD is used as a sensor for measuring fast electromagnetic pulse [9]. An attempt is made here to find out ideal profile of ACD antenna, which can be used as a feed for reflector IRA. The analysis results shows that ACD antennas with $\alpha > 0$ has better time domain response and good low frequency performance. As the ratio of point charge to line charge density (α) increases the girth of the ACD feed also increases, increasing the feed blockage of the antenna. Hence as an asymptotic conical dipole antenna, higher value of α is good but ACD used as a feed for reflector IRA, $\alpha = 0$ (only linear charge density) is ideal charge distribution used to generate ideal ACD profile. This ACD profile used as feed allows achieving smaller impedance value with smaller cone angle and smaller form factor. The ACD fed HIRA realized using the ideal profile is readily used with single-ended 50 Ω pulse generators and other measurement instrumentation.

6. CONCLUSION

The point charges used in the equivalent charge method improves the time domain response, particularly in late time because of reduced inductance. The increase in the girth of the dipole for the profiles with $\alpha > 0$ increases the feed blockage and hence $\alpha = 0$ is ideal ACD feed profile. The measured results of the ACD-fed HIRA show the suitability of novel feed for reflector IRAs.

REFERENCES

1. DuHamel R.H et al., “Frequency independent conical feeds for lens and reflectors,” in *proc. IEEE Int. Antennas Propagation Symp.* Dig.Vol.6, sep.1968, pp. 414-418.
2. Baum, C.E., “Radiation of Impulse-like Transient Fields,” Sensor and Simulation Note#321, 25 November 1989
3. Baum,C.E., and E.G Farr, “Impulse Radiating Antennas,” in *Ultra-wideband short Pulse Electromagnetics*, edited by H.L Bertoni et. Al, pp. 139-147, Plenum Press, NY 1993.
4. Baum,C E., “Configuration of TEM Feed for IRA”, Sensor and Simulation Note 327,27 April 1991.
5. Farr,E., “Optimizing the feed Impedance of Impulse Radiating Antenna,PartI:Reflector IRA”, Sensor and Simulation Notes 354, January 1993.
6. Farr.E, “Development of a Reflector IRA and a solid Dielectric Lens IRA”, Sensor and Simulation Note 396, April 1996.
7. M.Manteghi and Y.Rahamat-Sammii, “A novel Vivaldi fed reflector impulse radiating antenna (IRA),” in Proc. IEEE Int. Symp. Antennas and Propagation, Washington,DC, Jul.3-8,2005, pp. 549-552.
8. M.Manteghi and Y.Rahamat-Sammii, “On the characterization of a reflector impulse radiating antenna (IRA): Full-wave analysis and measurement results,” IEEE Trans. Antennas and Propagation, Vol.54, no.3, pp. 812-822, Mar2006.
9. Baum C E et al., “ Sensors for electromagnetic pulse measurements both inside and away from nuclear source regions,” IEEE Tran. Antennas and Propagation, Vol.26, pp. 22-35, Jan1978.
10. L. H Bowen et al., “A high voltage Cable feed impulse radiating antenna” in Ultrawideband short pulse electromagnetics8, edited by Baum et al., pp. 9-16, Springer, 2007.
11. D.V.Giri,"Peak Power Gain in time domain of Impulse Radiating Antenna (IRAs),” Sensor and Simulation Notes 546, October 2009.
12. Sower G.D., “Optimization of the asymptotic conical EMP sensors”, Sensor and Simulation Notes 295, Oct 1986.
13. C.E.Baum, “ An equivalent charge method for defining geometries of dipole antennas”, Sensor and Simulation Notes 72,Jan 1969.
14. D.V.Giri, “ High-Power Electromagnetic Radiators”, Harvard University Press, 2004.
15. Dhiraj Kumar Singh, D C Pande, and A. Bhattacharya, “A new feed for Reflector based 100Ω Impulse Radiating Antenna”, PIERS 2012,Malaysia, Mar 2012.

Appendix 'A'

Calculation of Surface potential for an infinite biconical structure is given below:

potential function is

$$\phi = \int_{-\infty}^{+\infty} \frac{\lambda(z')dz'}{4\pi\varepsilon_0 |\vec{r} - \vec{r}|}$$

$$\phi = \frac{1}{4\pi\varepsilon_0}\left\{\int_0^{\infty} \frac{\lambda(z')dz'}{[(z-z')^2+\psi^2]^{1/2}} + \int_{-\infty}^{0} \frac{\lambda(z')dz'}{[(z-z')^2+\psi^2]^{1/2}}\right\}$$

put $z' = -z''$

$$= \frac{1}{4\pi\varepsilon_0}\left\{\int_0^{\infty} \frac{\lambda(z')dz'}{[(z-z')^2+\psi^2]^{1/2}} + \int_{\infty}^{0} \frac{-\lambda(z'')(-dz'')}{[(z+z'')^2+\psi^2]^{1/2}}\right\}$$

Now for $z' > 0$

let λ *be a cons* tan *t* $\lambda_0 > 0$

this gives a step discontinuity in λ *of magnitude of* $2\lambda_0$ *at* $z' = 0$

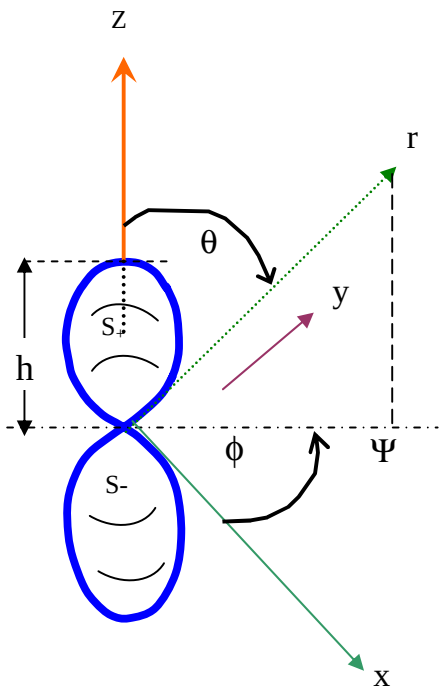

$$Let\ \eta_1 = \frac{z_1 - z}{\psi}, \eta_2 = \frac{z_1 + z}{\psi}$$

$$dz' = \psi d\eta_1, dz' = \psi d\eta_2$$

$$z' = 0$$

$$\eta_1 = \frac{-z}{4}, \eta_2 = \frac{z}{4}$$

$$z' = \infty \Rightarrow \eta_1 = \infty$$

$$\eta_2 = \infty$$

$$\phi = \frac{\lambda_0}{4\pi\varepsilon_0}\left[\int_{-z/4}^{\infty} \frac{(1+\eta_1{}^2)^{-1/2}.\psi d\eta_1}{\psi} - \int_{z/4}^{\infty} \frac{(1+\eta_2{}^2)^{-1/2}.\psi d\eta_2}{\psi}\right]$$

$$= \frac{\lambda_0}{4\pi\varepsilon_0} Lt_{v\to\infty}\left\{\int_{-z/4}^{\infty} (1+\eta_1^2)^{-1/2} d\eta_1 - \int_{z/4}^{\infty} (1+\eta_2)^{-1/2} d\eta_2\right\}$$

$$= Lt_{v\to\infty}\left\{\int_{-z/4}^{\infty} (1+\eta_1^2)^{-1/2} d\eta_1 + \int_{\infty}^{z/4} (1+\eta_2)^{-1/2} d\eta_2\right\}$$

$$= \frac{\lambda_0}{4\pi\varepsilon_0} Lt_{v\to\infty} \int_{-z/4}^{z/4} (1+\eta^2)^{-1/2} d\eta$$

$$= \frac{\lambda_0}{4\pi\varepsilon_0} \int_{-z/4}^{z/4} (1+\eta^2)^{-1/2} d\eta$$

$$= \frac{\lambda_0}{4\pi\varepsilon_0} x2\, Sinh^{-1}\left(\frac{z}{4}\right)$$

$$\phi = \frac{\lambda_0}{2\pi\varepsilon_0} Sinh^{-1}\left(\frac{z}{4}\right)$$

$$also = \frac{\lambda_0}{4\pi\varepsilon_0} x2\left[\ln\left(\frac{z}{4} + \left(1 + \left(\frac{z}{4}\right)^2\right)^{1/2}\right)\right]_0^{\frac{z}{4}}$$

$$\phi = \frac{\lambda_0}{2\pi\varepsilon_0}\left[\ln\left[\cot\left(\theta/2\right)\right]\right]$$

Setting $\phi = \phi_s$ to determine the upper antenna surface, and defining θ_0 as that value of θ for this surface so that

$$\phi_s = \frac{\lambda_0}{2\pi\varepsilon_0}\left[\ln\left[\cot\left(\theta/2\right)\right]\right]$$

Therefore biconical surface potential is

$$\phi_S = \frac{\lambda_0}{2\pi\varepsilon_0}\ln\left[\cot\left(\frac{\theta_0}{2}\right)\right]$$